High-Frequency Temperature and Humidity Correlation Above a Warm Wet Surface[1]

MARVIN L. WESELY AND BRUCE B. HICKS

Radiological and Environmental Research Division, Argonne National Laboratory, Argonne, Ill. 60439

(Manuscript received 10 June 1977, in final form 31 October 1977)

ABSTRACT

Temperature and humidity fluctuations at frequencies within the inertial subrange are found experimentally to be partially correlated in the surface boundary layer over warm wet surfaces. The spectral correlation coefficient, deduced from variances and covariances computed by analog electronics, is near unity in the flux-carrying eddies and decreases with increasing frequency, approximately as $n^{-\frac{1}{3}}$. As a result, optical refractive index fluctuations may have the false appearance of being strongly anisotropic in the inertial subrange.

1. Introduction

Temperature and humidity are among the quantities of a scalar nature that are most often studied in the atmospheric sciences, yet few data are available on the nature and extent of their correlation at high frequencies. In studies on the propagation of optical, acoustic, and radio waves in the lower atmosphere, the combined effects of temperature and humidity fluctuations can be influenced considerably by the extent of correlation between them (Wesely, 1976a). But evaluation of the correlation requires high-frequency sampling of humidity, which is known to be difficult, especially in the case where the sensor must be small and very close to a suitable thermometer in order to achieve a small sampling volume.

For the case of optical propagation in the surface boundary layer, effects such as image blurring and laser scintillation are usually caused by refractive index inhomogeneities of scale lengths less than 10 cm (e.g., see Tatarskii, 1971). At heights of 1 m, such scale lengths are associated with frequencies well within the inertial subrange. The sensors used to detect the corresponding temperature and humidity fluctuations should have adequate response up to 100 Hz and should be separated by less than 5 cm.

While recent measurements have shown that temperature and humidity fluctuations are almost perfectly correlated in the eddies carrying heat and water vapor vertically in unstable conditions over surfaces with considerable moisture available (Swinbank and Dyer, 1967; Phelps and Pond, 1971; McBean and Miyake, 1972; Thorpe *et al.*, 1973; Friehe *et al.*, 1975), the evidence on the degree of correlation at frequencies well within the inertial subrange in the surface boundary layer is incomplete. This paper will provide some relevant experimental evidence that could be applied in studies such as reported by Wesely (1976b), who used visual observations of image blurring to deduce line averages of the sensible heat flux over warm water surfaces. In this context, there is need for formulations relating the spectral correlation coefficient r_{eT} to the height z, mean wind speed $\bar{u}$ and cyclical frequency n, especially at the high frequencies beyond $f=nz/\bar{u}>2$.

2. Data collection techniques

Fluctuations of temperature and absolute humidity were measured above the surface of the warm cooling lake of the Dresden nuclear facility near Morris, Ill., and above vegetated land surfaces during the daytime. Fig. 1 shows the two sensors as used above the cooling pond. Each has a sampling length of less than 1 cm and the sensors are separated by less than 3 cm at the extreme edges of the sampling volumes. The thermometer is a platinum resistance wire about 2 μm in diameter, with a time response less than 0.2 ms when exposed to moving air. The thermometer is very near the sensing gap of a Lyman-alpha hygrometer, which was modified by fitting a pair of lenticular venturis around the gap, as shown in Fig. 1. This modification ensured that no blunt surfaces interfered with the air flow to the sensed region. The same instrumentation was used above the land surfaces, except that smaller venturis were used and the thermometer was placed 3.5–12.7 cm upwind of the hygrometer sensing gap.

At the cooling lake, the instruments were placed on a mast that was attached to a rigid platform located in

[1] This work was supported by the U. S. Department of Energy.

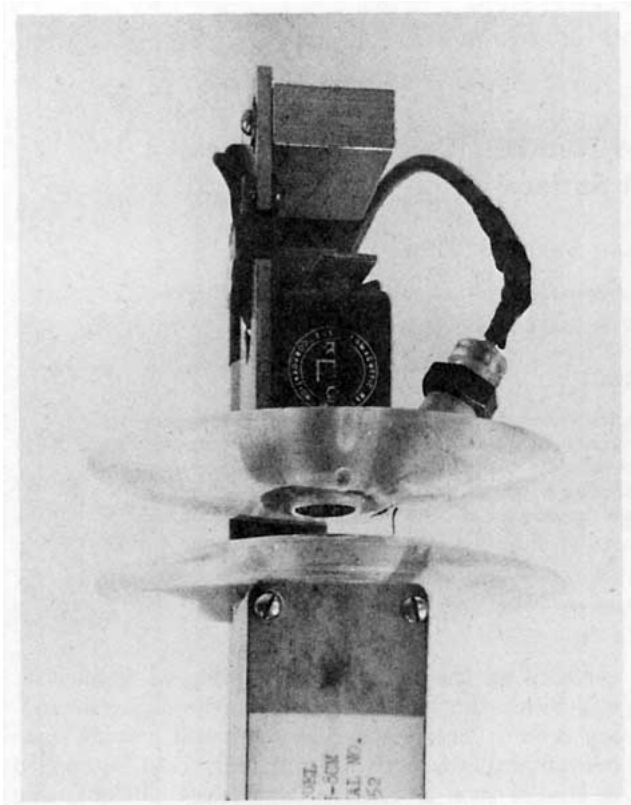

FIG. 1. The Lyman-alpha hygrometer and fine-wire resistance thermometer mounted near the sensing gap of the hygrometer. The Lyman-alpha radiation passes vertically through a circular window at the center of the lower disk, and the resistance wire is suspended between the supports that can be seen between the two disks.

the center of the warmest of several pools, while most of the electronic apparatus was operated on a pontoon boat downwind. Since advection can be severe in the circumstance of a pond bordered by rougher land or cooler pools, precautions were taken to ensure that fetch-to-height ratios were at least 400:1. A more detailed description of the pond site and some related experimental procedures have been given elsewhere (Wesely, 1976b). The land surfaces employed were fields of grass and soybeans, both of which were green and well supplied with soil moisture.

The thermometer was operated in a direct current resistance bridge which produced an output of about 0.5 V $°C^{-1}$; the hygrometer circuitry used produced approximately 0.2 V/(g H_2O/kg air). These signals were fed to RC high pass filters and variable-gain amplifiers, and then to analog multipliers and squaring circuits similar to those used in portable covariance meters (Hicks, 1970). A single "correlation meter" contained all of the needed filters, amplifiers, and multipliers, as well as panel meters to display the results. In operation, input signals to the correlation meter were switched to selected capacitors in order to vary the time constant τ of the high pass filter and thus the parameter $\mathcal{T}=z/(\tau\bar{u})$, where $\bar{u}$ is the mean wind speed and z is the height of measurement. Gains were also adjusted in the field so that signal-to-noise ratios were large, even with the greatest amount of filtering employed. Of course, at all possible gains and filter values, identical signals in both inputs of the correlation meter resulted in correlation coefficients of unity.

Ordinarily, to compute the spectral correlation coefficient,

$$r_{eT}(n)=C_{eT}(n)[S_e(n)S_T(n)]^{-\frac{1}{2}}, \quad (1)$$

the temperature spectrum $S_T(n)$, the water vapor pressure spectrum $S_e(n)$ and the cospectrum $C_{eT}(n)$ would be determined. This would provide a direct measurement of the desired quantity and would also indicate if the high-frequency fluctuations of temperature and humidity behave as expected according to the familiar $-5/3$ slope in the inertial subrange. However, the analog method provided only an integral correlation coefficient $R_{eT}(\mathcal{T})$, which is simply the correlation coefficient for all of the temperature and humidity fluctuations except those removed by the high pass filtering. The advantages of this approach are 1) easy deployment of electronics on a pontoon boat on which only small low-power devices could be used, 2) rapid evaluation and inspection of results, and perhaps most important, 3) the capability to readjust gains during the experiment so that maximum usable signals can be obtained at each value of the high pass filter selected. We believe that large signal-to-noise ratios are crucial to the success of such an experiment. The noise levels at high amplifications were checked in the field by placing the instruments in a small chamber in which the fluctuations of temperature and humidity were extremely low. Because the amplifications were frequently changed without precise calibration when the input filters were altered, no checks on the high frequency roll-off of the variances of the signals were obtained. Thus, information that would have led to some measure of raw spectral or cospectral estimates was not collected, forcing several assumptions to be made about spectra and cospectra in order to permit an evaluation of $r_{eT}(n)$.

3. Assumptions and derivations

The main assumptions needed to interpret the field data are that the spectra of temperature and humidity fluctuations and their cospectra have universal shapes when properly scaled for conditions in the surface boundary layer, and that certain continuous mathematical functions can be used to describe those shapes. A starting point is provided by the expression given by Kaimal *et al.* (1972) for temperature spectra in near-

neutral conditions,

$$nS_T(n)/T_*^2 = \begin{cases} 53.4f/(1+24f)^{5/3}, & f \leqslant 0.15 \\ 24.4f/(1+12.5f)^{5/3}, & f > 0.15 \end{cases} \quad (2)$$

where $f=nz/\bar{u}$ is the normalized frequency and $T_*=\overline{w'T'}/u_*$ is a temperature scaling parameter in the surface boundary layer. (The term w represents vertical wind speed, T potential temperature, and u_* surface friction velocity; the primes indicate deviations from the mean and the overbar a time average.) Eq. (2) is meant to describe near-neutral conditions rather than the unstable conditions that existed over the Dresden cooling pond during the measurements; the magnitudes of the normalized spectral values at low-frequencies are known to increase as the instability increases. However, since the high pass filtering employed should eliminate the contributions of the low frequency fluctuations to the variances and covariances measured, use of (2) should be as sufficient as more complete formulations, in the present applications.

As will be shown later, the value of R_{eT} is near unity when the value of $\mathcal{T}$ is near 1. It will be evident that this implies that r_{eT} is also near unity for frequencies associated with eddies that carry heat and water vapor vertically. This inference is consistent with findings of investigators mentioned in the Introduction. Further, at higher frequencies the humidity fluctuations result from variations transmitted from the flux-carrying eddies by processes that are similar to those for temperature fluctuations. Such considerations lead us to assume that temperature and humidity spectra have the same shape at flux-carrying and inertial-subrange frequencies. Thus, we can write

$$S_e(n)/\sigma_e^2 \approx S_T(n)/\sigma_T^2, \quad (3)$$

$$C_{eT}(n) \approx r_{eT}(n)\sigma_e S_T(n)/\sigma_T, \quad (4)$$

where σ_e and σ_T are the standard deviations of vapor pressure and temperature variations, respectively, not subjected to filtering. Henceforth in this paper S_T and S_e will be used interchangeably as specified by (3).

The parameter $\mathcal{T}=z/(\tau\bar{u})$ represents τ^{-1} normalized for various values of $\bar{u}$ and z, similar to the manner in which $f=nz/\bar{u}$ is commonly employed to represent normalized frequency. With use of standard expressions for the high pass RC electrical filters, the spectrum of the signal transmitted to the multiplier circuits of the correlation meter can be found to be

$$s_T(n,\tau) = S_T(n)\{1-[1+(2\pi n\tau)^2]^{-1}\}, \quad (5)$$

which is equivalent to

$$s_T(n,\tau) = S_T(n)\{(2\pi f/\mathcal{T})^2[1+(2\pi f/\mathcal{T})^2]^{-1}\}. \quad (6)$$

Similar expressions for $s_e(n,\tau)$ and $c_{eT}(n,\tau)$ that incorporate the effects of high pass filtering can be found for humidity spectra and temperature and humidity cospectra, respectively.

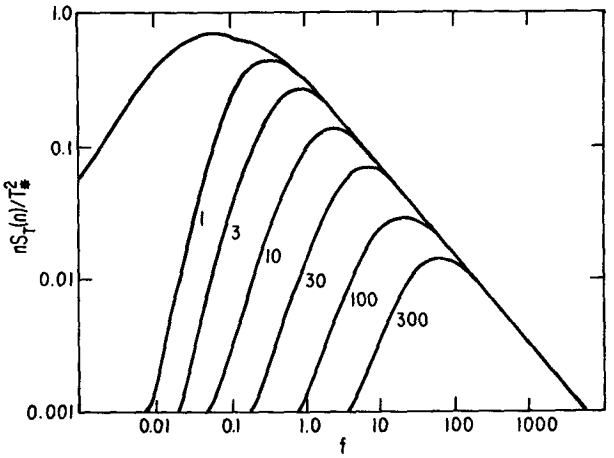

FIG. 2. A normalized temperature spectrum (after Kaimal *et al.*, 1972) and the change in the spectrum after high-pass filtering with various values of $\mathcal{T}$, as calculated by use of (6).

Fig. 2 shows the effects of filtering as given by (6). It is evident that perhaps for $\mathcal{T}>10$ and certainly for $\mathcal{T}>30$, only the fluctuations for $f>1$, where $S_T(n)$ obeys a $-5/3$ power law, contribute significantly to the signals transmitted to the multiplier circuits in the correlation meter. Hence, for large values of $\mathcal{T}$ only fluctuations associated with inertial subrange frequencies give rise to the variances and covariances computed by use of the correlation meter.

It is important to express τ, which determines R_{eT}, directly in terms of n, which determines r_{eT}, so that a one-to-one correspondence between R_{eT} and r_{eT} can be established. The effect of high pass filtering of inertial subrange fluctuations by use of a certain time constant τ_0 (or $\mathcal{T}_0$) is to isolate, although somewhat imperfectly, most of the fluctuations at frequencies greater than a particular value n_0 (or f_0). Expressed mathematically for temperature fluctuations, this implies that a value n_0 can be found such that the following is valid:

$$\int_{n_0}^{\infty} S_T(n)dn = \int_0^{\infty} s_T(n,\tau_0)dn. \quad (7)$$

In the inertial subrange, $S_T(n)$ is proportional to $n^{-5/3}$. With use of this proportionality and (6), both sides of (7) can be integrated for the case of the inertial subrange to yield

$$n_0 = [3\pi^{-1}\sin(2\pi/3)]^{\frac{3}{2}}/(2\pi\tau_0), \quad (8)$$

or

$$\mathcal{T}_0 = 8.36 f_0. \quad (9)$$

These relations imply that a small difference $\Delta\mathcal{T}$ centered on $\mathcal{T}_0$ can be used to yield a small change $\Delta R_{eT}(\mathcal{T}_0)$ that bears a single valued and continuous relationship to $r_{eT}(f_0)$ in the inertial subrange.

The normalized integral $I(\tau)$ of either temperature or humidity fluctuations after high pass filtering can

be expressed as

$$I(\tau)=\sigma_T^{-2}\int_0^\infty s_T(n,\tau)dn. \tag{10}$$

Considerations involving integration of $c_{eT}(n,\tau)$ over all positive frequencies and use of (3) and (4) result in a simplification of the definition

$$R_{eT}(\tau)\equiv\int_0^\infty c_{eT}(n,\tau)dn \times\left[\int_0^\infty s_e(n,\tau)dn\int_0^\infty s_T(n,\tau)dn\right]^{-\frac{1}{2}}, \tag{11}$$

that is,

$$R_{eT}(\tau)I(\tau)=\sigma_T^{-2}\int_0^\infty r_{eT}(n)s_T(n,\tau)dn. \tag{12}$$

All of the functions within the integrals of (10) and (12) are continuous functions of n or of n and τ, and are assumed to have values of the same sign throughout the entire range of n. Thus, the functions I and R_{eT} are extremely well behaved mathematically, i.e., they are continuous single-valued functions of τ for given values of $\bar{u}$ and z. As a result, we can consider R_{eT} to be a function of I, provided r_{eT} changes monotonically with increasing n. Combined with the assumptions that $R_{eT}=R_{eT}(I(\mathcal{T}))$ and $I=I(\mathcal{T})$, application of fundamental integral and differential calculus leads us to a simple expression for r_{eT}:

$$r_{eT}(f)=R_{eT}+I\frac{dR_{eT}}{d\mathcal{T}}\Big/\frac{dI}{d\mathcal{T}}, \tag{13}$$

where, as shown by (9), f on the left hand side bears a direct relationship to the value of $\mathcal{T}$ that specifies the functions R_{eT} and I on the right hand side.

To further simplify (13), (7) can be substituted into (10), the variable in the limits of the integral can be changed from n_0 to $\mathcal{T}_0$, and the assumption that $S_T(n)$ is proportional to $n^{-5/3}$ can be used. This leads to the expression

$$I\Big/\frac{dI}{d\mathcal{T}}=-(\tfrac{3}{2})\mathcal{T}. \tag{14}$$

This expression can be substituted into (13) to yield the relationship

$$r_{eT}(f)=R_{eT}(\mathcal{T})-(\tfrac{3}{2})\mathcal{T}\frac{dR_{eT}(\mathcal{T})}{d\mathcal{T}}, \tag{15}$$

which together with (9) forms the main result of this section.

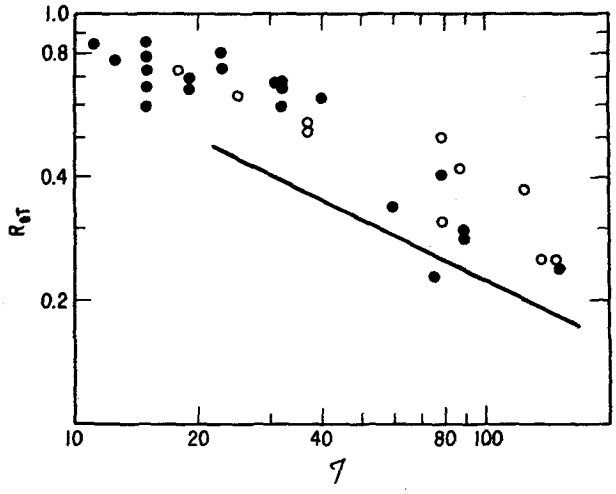

FIG. 3. Experimental values of the integral correlation coefficient R_{eT}. Measurements taken at 0.5–1.3 m above the water surface are indicated by solid dots, and those taken at 11.5 m above grass by open circles. The solid line has a slope of $-\frac{1}{2}$.

4. Results and discussion

Fig. 3 shows a plot of the experimentally determined correlation of temperature and humidity fluctuations. For $\mathcal{T}\gtrsim 30$, eleven data points were obtained during three different days at heights of 0.52–1.32 m above the water surface. A regression performed with these data results in the power relationship

$$R_{eT}=8.5\mathcal{T}^{-0.74}, \tag{16}$$

with a standard error of ± 0.09 on the value of the exponent.

It is evident that the correlation between temperature and humidity for the low-frequency anisotropic fluctuations corresponding to the left hand side of Fig. 3 is quite large, while near the high-frequency end of Fig. 3 where viscous effects are important, "randomization" of the fluctuations results in little correlation. Numerous measurements at $0.1<\mathcal{T}<10$ provide a nearly constant value of about 0.95 for R_{eT}.

By use of (9) and (15), expressions for r_{eT} can be derived. Corresponding to (16) is the relationship

$$r_{eT}=3.7f^{-0.74}. \tag{17}$$

The sign and the maximum magnitude of r_{eT} can be substantially different over other surfaces. For example, over a cool water surface where the vertical gradients of mean temperature and humidity are of opposite sign, r_{eT} is negative (Friehe *et al.*, 1975). Measurements over land indicate that when the surface temperature is very near air temperature or when moisture is not readily available at a land surface, the maximum magnitude of r_{eT} can be much less than unity (McBean and Miyake, 1972; McBean, 1973).

To determine the reliability of the results from cooling pond studies and to investigate the case in which

TABLE 1. Measurements of R_{eT} during the daytime over green vegetation. The values of $\hat{R}_{eT}$ are those for R_{eT} divided by 0.37 for case 1, and by 0.26 for case 2. For comparison to the cooling pond results, the heights of the instruments above the water surface were 0.5–1.5 m and the values of $D(\tau\bar{u})^{-1}$, where D is the separation distance between thermometer and hygrometer, were 2–5 when $\mathcal{T}$ was greater than 100.

Case	z (m)	$\bar{u}$ (m s^{-1})	τ (s)	$\mathcal{T}$	$D(\tau\bar{u})^{-1}$	R_{eT}	$\hat{R}_{eT}$	$8.5\mathcal{T}^{-0.74}$	$2.5\mathcal{T}^{-0.43}$
1	11.5	3.5	3.0	1.1	0.01	0.35	0.95	—	—
	11.5	3.5	0.15	22	0.19	0.29	0.79	—	—
	11.5	3.5	0.071	47	0.41	0.21	0.57	0.49	0.48
	11.5	3.5	0.033	100	0.87	0.14	0.36	0.28	0.35
2	4.0	3.0	0.15	8.9	0.08	0.25	0.95	—	—
	4.0	2.9	0.071	20	0.17	0.21	0.79	—	—
	4.0	3.0	0.033	40	0.35	0.14	0.56	0.55	0.51
3	11.5	4.2	0.15	18	0.16	0.73		—	—
	11.5	3.1	0.15	25	0.08	0.63		—	—
	11.5	4.4	0.071	37	0.11	0.52		0.59	0.53
	11.5	4.4	0.071	37	0.32	0.54		0.59	0.53
	11.5	3.3	0.071	50	0.15	0.37		0.47	0.46
	11.5	4.4	0.033	78	0.24	0.52		0.34	0.38
	11.5	2.0	0.033	79	0.88	0.32		0.34	0.38
	11.5	4.0	0.033	87	0.78	0.42		0.31	0.37
	11.5	2.8	0.033	125	0.37	0.38		0.24	0.31
	11.5	2.5	0.033	137	1.6	0.25		0.22	0.30
	11.5	2.3	0.033	149	0.45	0.25		0.21	0.29

the maximum magnitude of r_{eT} (or R_{eT}) is considerably less than unity, a supplemental body of data has been collected over vegetated surfaces. Table 1 shows the results. Cases 1 and 3 were obtained at one site which had a surface mostly covered with green grass and bushes. For case 1 the measurements were taken during the afternoon of a day when the soil was only moderately moist. For case 3 the soil was quite moist, as a result of recent rains, and furthermore the measurements were taken in the morning when some dew was still present. Cases 1 and 3 evidently support the contention that ready availability of both moisture and heat at the surface is needed in order to produce large values of R_{eT}. Further, when R_{eT} at each value of $\mathcal{T}$ is divided by the value of R_{eT} expected by extrapolation to where $\mathcal{T}\approx 1$, conformity with (16) is found, suggesting that the relative rate of destruction of correlation between temperature and humidity fluctuations in the inertial subrange is independent of the maximum amount of correlation. Case 2, taken over soybeans in midseason during the afternoon, verifies this result.

Table 1, especially case 3, provides an important check on (16). Fig. 3 also shows the data from case 3. The values of τ employed at a height of 11.5 m were nearly ten times greater than those employed at 0.5–1.5 m above the cooling pond, for given values of $\mathcal{T}$. Thus, some possible sources of error that could introduce an erroneously large rate of decrease of R_{eT} with increasing $\mathcal{T}$ are not as likely to be of serious consequence as they might have been over the cooling pond. For example, attenuation due to limited frequency responses of electronics or sensors, to spatial separation of sensors, or to large sensor size could have lowered the values of R_{eT} at large $\mathcal{T}$, but a factor of ten increase in height reduces substantially the crucial requirements. For the data with $\mathcal{T}>30$ in case 3, the correlation coefficient is

$$R_{eT}=2.5\mathcal{T}^{-0.43}, \tag{18}$$

which implies the spectral form

$$r_{eT}=1.6f^{-0.43}, \tag{19}$$

where the standard error on the exponent in (18) is ± 0.13.

As shown in Table 1, (18) and (16) produce very similar results except for values of $\mathcal{T}$ greater than about 100 where, as shown by the relatively large scatter in Fig. 3, the data are least reliable. Nevertheless, on the basis of the exponents in (18) and (16), it appears that signal attenuation may have been significant at high frequencies for the measurements over water. Sensor spacing or size may have been the cause of the attenuation. Whatever the cause, the true exponent, if one exists, is most likely nearer -0.43 than -0.74. A value of $-\frac{1}{2}$ for the exponent seems a reasonable choice, considering the uncertainties associated with instrument separation distance and sampling size. Further measurements are needed to improve confidence in this regard.

5. Conclusions

The final results given by (18) and (19) indicate that in the surface boundary layer over wet surfaces, tem-

perature and humidity fluctuations are partially correlated in the inertial subrange, varying from highly correlated in the eddies that carry heat and moisture vertically, to almost zero correlation at the scales where dissipation of temperature and humidity inhomogeneities takes place. The exact form of the variation of r_{eT} with frequency cannot be determined with the experimental methods used here, but the average slope of r_{eT} versus frequency on a log-log plot is approximately $-\frac{1}{2}$. These results suggest that the structure function coefficients for the optical refractive index in the atmosphere at a given height above the surface may vary in a way depending on the scale lengths associated with the scattering.

The one-dimensional power spectrum of optical refractive index fluctuations can be expressed as

$$\Phi(\kappa)=0.25C_n^2\kappa^{-5/3}, \tag{20}$$

where κ is the wave-number component in the streamwise direction. An expression for the refractive index structure-function coefficient C_n^2 in the notation of Wesely (1976a), as derived from his Eq. (9), is

$$C_n^2=C_T^2A_1^2p^2T^{-4}+r_{eT}C_TC_epA_1[T^3(A_1-A_2)]^{-1}+C_e^2[T^2(A_1-A_2)^2]^{-1}. \tag{21}$$

Since r_{eT} is a function of f, and thus of $\kappa=2\pi f/\bar{u}$ (by Taylor's hypothesis), the result of substituting (21) into (20) implies that $\Phi(\kappa)$ is actually not simply proportional to $\kappa^{-5/3}$. This seems to contradict the argument that fluctuations of refractive index in the inertial subrange are isotropic, because the fluctuations of temperature and humidity are assumed to be isotropic in order to find theoretically that their spectra should be proportional to $\kappa^{-5/3}$ (Obukhov, 1949; Corrsin, 1951). However, for a nonconservative quantity such as refractive index, it is not required that C_n^2 be constant for isotropy to exist. Hence, the findings in this paper do not necessarily support the contention that a varying amount of correlation between temperature and humidity fluctuations negates the often used assumption that fluctuations of refractive index are isotropic at frequencies corresponding to the inertial subrange.

The expressions for r_{eT} in this paper may be useful in studies involving acoustic and microwave propagation in the atmosphere. Since the value of r_{eT} is quite low at frequencies $f\simeq 50$, it may be justifiable to assume that the magnitude of r_{eT} is zero for frequencies corresponding to temperature and humidity inhomogeneities at scale lengths less than 1 m when $z/\bar{u}$ is large, such as in the upper surface boundary layer or above. Indeed, acoustic waves and microwaves currently used in remote sensing schemes are often of such wavelengths that refractive index inhomogeneities less than 1 m in length are most effective in producing useful measures of the structure of the planetary boundary layer.

Acknowledgments. The modification of the commercially available Lyman-alpha hygrometer was designed by P. Frenzen. Eqs. (9) and (15) were derived with the assistance of R. G. Everett.

REFERENCES

Corrsin, S., 1951: On the spectrum of isotropic temperature fluctuations in an isotropic turbulence. *Appl. Phys.*, **22**, 469–473.

Friehe, C. A., J. C. LaRue, R. H. Champagne, C. H. Gibson and G. F. Dreyer, 1975: Effects of temperature and humidity fluctuations on the optical refractive index in the marine boundary layer. *J. Opt. Soc. Amer.*, **65**, 1502–1511.

Hicks, B. B., 1970: The measurement of atmospheric fluxes near the surface: A generalized approach. *J. Appl. Meteor.*, **9**, 386–388.

Kaimal, J. C., J. C. Wyngaard, Y. Izumi and O. R. Coté, 1972: Spectral characteristics of surface-layer turbulence. *Quart. J. Roy. Meteor. Soc.*, **98**, 563–589.

McBean, G. A., 1973: Comparison of the turbulent transfer processes near the surface. *Bound.-Layer Meteor.*, **4**, 265–274.

——, and M. Miyake, 1972: Turbulent transfer mechanisms in the atmospheric surface layer. *Quart. J. Roy. Meteor. Soc.*, **98**, 383–398.

Phelps, G. T., and S. Pond, 1971: Spectra of the temperature and humidity fluctuations and of the fluxes of moisture and sensible heat in the marine boundary layer. *J. Atmos. Sci.*, **28**, 918–928.

Obukhov, A. M., 1949: Structure of the temperature field in turbulent streams. *Izv. Akad. Nauk. SSSR Ser. Geofiz.*, **13**, 58–69.

Swinbank, W. C., and A. J. Dyer, 1967: An experimental study in micrometeorology. *Quart. J. Roy. Meteor. Soc.*, **93**, 494–500.

Tatarskii, V. I., 1971: *The Effects of the Turbulent Atmosphere on Wave Propagation.* (Israel Program Scientific Translation) NOAA TT 68-50464, 471 pp. [Available from NTIS].

Thorpe, M. R., E. G. Banke and S. D. Smith, 1973: Eddy correlation measurements of evaporation and sensible heat flux over Arctic sea ice. *J. Geophys. Res.*, **78**, 3573–3584.

Wesely, M. L., 1976a: The combined effect of temperature and humidity fluctuations on refractive index. *J. Appl. Meteor.*, **15**, 43–49.

——, 1976b: A comparison of two optical methods for measuring line averages of thermal exchanges above warm water surfaces. *J. Appl. Meteor.*, **15**, 1177–1188.